Research Article | Vol. 27, No. 21 / 14 October 2019 / Optics Express 29547
Optics EXPRESS

Highly flexible electrochromic devices enabled by electroplated nickel grid electrodes and multifunctional hydrogels

SHI-QING ZHAO,[1] YAN-HUA LIU,[1,3] ZHU MING,[1] CHENG CHEN,[1] WEN-WEN XU,[1] LINSEN CHEN,[1] AND WENBIN HUANG[1,2,4]

[1]School of Optoelectronic Science and Engineering & Collaborative Innovation Center of Suzhou Nano Science and Technology, Soochow University, Suzhou, 215006, China
[2]State Key Lab of Applied Optics, Changchun Institute of Applied Optics, Fine Mechanics and Physics, Chinese Academy of Sciences, Changchun, Jilin, 130033, China
[3]yhliu@suda.edu.cn
[4]wbhuang@suda.edu.cn

Abstract: Flexible electronics, as a futuristic technology, is presenting tremendous impact in areas of wearable displaying, energy saving, and adaptive camouflage. In this work, we constructed a simple triple-layered electrochemical device with high flexibility using the electroplated nickel (Ni) grid electrode and the multifunctional hydrogel. The Ni grid electrode with low resistance (0.5 Ω/sq), high optical transparency (84.8%) and good mechanical flexibility, is beneficial for efficient electron injection, while the transparent lithium chloride hydrogel functions simultaneously for ion storage, ion transportation and counter-conducting. The thin polymer poly(3,4-ethylenedioxythiophene): poly(styrenesulfonate) (PEDOT: PSS) film is utilized as the electrochromic (EC) material and it also distributes the electrons evenly for uniform coloration. The triple-layered EC architecture not only simplifies the manufacturing procedures but also improves the device performance in terms of optical contrast and mechanical robustness. The device shows fast response for coloration and bleaching with an absolute transmittance contrast of 40% and a contrast retention over 72% after 2500 bending cycles. The ability of the flexible electrochromic device for conformable attaching was also investigated without obvious performance degradation. The electroplated Ni grid electrode and the multifunctional hydrogel are advantageous in constructing flexible electrochromic devices in terms of the response time, the working stability and the bending capability, paving a way for next-generation flexible electronics.

1. Introduction

The development of flexible, lightweight, inexpensive and low-power deformable electronics is in urgent need as a futuristic technology, opening the possibility for diverse applications such as wearable electronics, adaptive camouflage and biomimicry [1,2]. Optoelectronic devices that dynamically alter their response in terms of the absorption/reflection/scattering spectrum under the application of a suitable electric potential are known as electrochromic devices (ECDs) and are attracting tremendous attention for practical applications [3]. Smart windows based on ECDs are valued for their aesthetic glazing and low energy consumption, which can reduce glare or visible/infrared irradiation on demand [4,5], have found widespread applications as architectural building windows, auto-dimming rear view mirrors, and military camouflage surfaces. In addition, the ECD has also positioned itself as one of the potential candidates for the next-generation displays, owing to features such as low-power consumption, wide viewing angles, high angle-independent contrast, and good coloration memory effects [6,7]. The basic prerequisite of an EC material is the reversible electrochemical redox behaviour, with the ability to undergo color switching through intercalation or de-intercalation of ions and injection or

#371801 https://doi.org/10.1364/OE.27.029547
Journal © 2019 Received 8 Jul 2019; revised 15 Sep 2019; accepted 19 Sep 2019; published 30 Sep 2019

Optics EXPRESS

extraction of electrons with the exertion of electrical bias [8]. ECDs share the multi-layered structure which commonly consists of the transparent conducting electrode, the electrochromic material, the electrolyte, the ion storage layer and the counter conducting electrode, and it holds the potential for flexible electronics as long as the multi-layered ECD structure was made flexible, which requires a careful design of every component to be flexible and transparent [9].

To this regard, the flexible conducting electrode (TCE) with high transparency and low sheet resistance is an important factor in realizing high performance ECDs. Flexible ECDs have already been constructed using polyethylene terephthalate (PET) substrates coated with tin-doped indium oxide (ITO) as the TCE from inorganic EC materials [10–12]. Further, a multi-colored flexible ECD was demonstrated from a solution-processable electroactive aromatic polyimide on the ITO flexible substrate [13]. However, ITO suffers from intrinsic brittleness, scarcity of indium, and difficulty in getting conformal large-area coatings, which renders it not applicable for extremely flexible and large-area ECD applications [14,15]. The PEDOT:PSS film owning better compatibility with organic EC materials was used as the TCE to form all-polymer ECDs with better flexibility [16] and the polymer surface was modified with surfactants to improve the conductivity and the conducting potential window properties for high performance flexible ECDs [17], however, limited successes were achieved due to its low conductivity and high redox activity in the working potential window [18]. The Ag nanowire network with intrinsically good conductivity and mechanical compliance has been successfully transferred onto the PET [19], polydimethylsiloxane (PDMS) substrates [20,21] and adopted as the conductive layer to demonstrate large-area, flexible and stretchable ECDs. In addition, the robustness of the Ag nanowire network could be improved via the co-assembly with tungsten oxide or carbon nanotube nanowires on flexible PET [22] or cellulose [23] substrates, however, Ag is electrochemically unstable and prone to oxidation, and additional processing procedures such as UV or thermal sintering and overcoating the protective reduced graphene oxide layer are often required [24–28], which add manufacturing complexity and cost. On the other hand, the metal grid which has advantages of high transparency, conductivity and flexibility, is emerging as the high performance TCE to build flexible ECDs, where the blooming effect would be solved with an additional polymer conducting layer. To date, silver and gold grids resulting from the self-assembling [29–32], flexographic printing [33,34] and patterned etching [35] techniques have been successfully utilized to construct flexible ECDs, however, new fabrication techniques with potential to yield metal grids with volume manufacturing, excellent photoelectric properties and high stability are still in demand for building high performance flexible ECDs.

Another major limitation for a flexible ECD is the complex five-layered architecture that supports the injection and extraction of corresponding ions and electrons in the EC material [36]. For example, as the solid electrolyte often suffers from low ionic conductivities and high interfacial charge transfer resistances, the multiple interfacial layers render the ion transportation even more difficult and thus deteriorate the device performance. In addition, solid electrolytes commonly have poor contact with the other layers, resulting in detachment or dislodgement of the function films during external deformations in long-term operations. Ionic hydrogels are considered as an excellent transparent electrode material with combined advantages of high transmittance, low resistance, biocompatibility and mechanical flexibility [37]. Furthermore, the liquid electrolyte could reside in the 3D polymer network structure which allows the hydrogel to serve as ion storage medium and simultaneously facilitates ion transportation via the continuous 3D channels. To date, simplified ECDs with the hydrogel layer acting tri-functions of ion transportation, ion storage and counter-conducting have been constructed in the liquid state [38] or on the fluorine-doped tin oxide (FTO) electrode [39], and further investigations into flexible ECDs based on the multifunctional hydrogel are of importance, as the simple ECD may pave a new approach for high performance conformal or wearable electronics.

Optics EXPRESS

In this work, we constructed a highly flexible ECD based on the electroplated Ni grid electrode and a multifunctional hydrogel. The electroplated Ni grid electrode bearing very low sheet resistance (0.5 Ω/sq), high transmittance (84.8%), and high flexibility functions as the supporting motif for efficient electron injection, where the PEDOT: PSS layer homogenizes the electric field across the film and experiences reversible redox reactions for electrochemical purposes. The hydrogel with both good film-forming and high charge transfer abilities simultaneously serves as the counter transparent electrode, the electrolyte and the ion storage layer, which is utilized to complete the highly flexible solid-state ECD with good switching performance and long-term stability.

2. Experimental details

2.1. The Ni transparent electrode fabricated by confined electroplating

The fabrication of the Ni transparent electrode with a high figure of merit consists of two procedures of lithography and electroplating [40]. The grid pattern was first written into the photoresist on the ITO substrate by the laser direct write technique where the linewidth could be as narrow as 2 μm and arbitrary grid patterns aiming for different applications could be easily achieved. Then the Ni metal filled in the photoresist micro-grooves by means of electroplating where the exposed ITO regions served as the patterned electroplating electrode. After that, the photoresist was removed and the UV-curable resin (D10, Phichem) was drop-casted onto the substrate, followed by fixing a flexible polyethylene terephthalate (PET) (thickness around 20 μm) onto the UV resin through a roll-to-roll process. Finally, the UV resin was cured under UV light (1000 mW/cm^2, Led Lamplic) for 25 s and the PET substrate was peeled off from the ITO substrate with the Ni grid electrode embedded in the cured resin on it.

2.2. Preparation of the multi-functional hydrogel

Acrylamide monomer (AAM, 0.8 g, Beijing Innochem Technology) was first added into 5 ml deionized water and magnetically stirred for 15 minutes. Subsequently, lithium chloride (LiCl, 1.1 g, Beijing Innochem), ammonium persulfate (AP, 13 mg, Shanghai Aladdin Biochem), methylene double acrylamide (MBAA, 4.7 mg, Shanghai Aladdin Biochem), and tetramethyl ethylenediamine (TEMED, 2 mg, Beijing Innochem) were added into the solution consecutively and the mixture was magnetically stirred for 2 h at room temperature to obtain a homogeneous solution. After that, the solution was put into the vacuum oven for 1 h to remove the bubbles. Finally, the solution was transferred into a plastic mold and heated at 60 °C using a hot plate for 1 h to yield the cross-linked hydrogel.

2.3. The assembly of the ECDs

PEDOT: PSS solution (10 ml, 0.8 wt% PEDOT, 0.5 wt% PSS, Heraeus Deutschland GmbH & Co. KG) was added with ethylene glycol (0.7 g, Shanghai Aladdin Biochem) and surfactant (Triton-X100, 0.025 g, Shanghai Aladdin Biochem) and sonicated for 15 min to form a stable mixture. The Ni grid transparent film was then treated with oxygen plasma to improve the surface hydrophilic property and was spin-coated with the prepared PEDOT: PSS mixture at a rotation speed of 3000 rpm for 30 s, and was subsequently annealed at 120 °C for 20 min for solution evaporation and morphology improvement. The PEDOT: PSS film functions as the EC material and also planarizes the electric-field in the triple-layered device architecture. After that, the hydrogel film was cut into rectangles and was placed onto the PEDOT: PSS film owing to its intrinsic compliance, completing the flexible transparent electrochromic device with a very simplified triple-layered architecture.

Optics EXPRESS

2.4. Characterization

The surface morphology and elemental analysis of the Ni grid electrode/PEDOT: PSS composite film was carried out with the field emission scanning electron microscopy (SEM) (JEOL, JSM-5400, USA). The thickness of the spin-coated PEDOT: PSS films and sheet resistance the electroplated Ni grid electrodes were measured by a step profiler (XP-200, Ambios Technology) and a four-point probe (CMT SR2000, A. I. T.), respectively. Electrochromic properties and electrochemical behaviors were measured on a UV-VIS spectrophotometer (SPECORD 210 PLUS, Analytikjena) and an electrochemical workstation (CHI 760E, Shanghai CH Instrument), respectively.

3. Results and discussion

The simplified ECD structure is shown in Fig. 1(a) which consists of the Ni grid electrode for efficient electron injection, the PEDOT: PSS layer for electrochemical reactions and the multifunctional hydrogel for ion transportation, ion storage and counter-conducting. The thickness of the Ni grid was around 4 μm and was embedded in UV resin on the flexible substrate with a very small height difference to the upper surface of the UV resin, giving rise to ultra-high robustness. In addition, the organic nature of other thin films ensures both good mechanical flexibility and interfacial compatibility, which are beneficial for reliable operation of the device under repeated bending or conformal attaching circumstances. Figure 1(b) shows the SEM image of the Ni grid embedded in the substrate and it is a honeycomb pattern with a linewidth of 4 μm and a diagonal length of 100 μm. The optical loss caused by the diffraction of the Ni grid is low (below 5%) and could be further reduced by redesigning the grid into a random pattern. The grid pattern and the distribution of the grid line could be designed and realized on demand. The Ni grid electrode appears quite transparent and merely influences the observation of a flower when placed in front of it (Fig. 1(c)) due to the low metal aspect ratio, thereby providing a high transmittance. The blooming effect caused by the Ni grid electrode is solved by the EC material PEDOT: PSS, where the metal grid functions the motif for fast electron injection while the polymer conducting film distributes the electrons across the whole plane for homogeneous coloration. The PEDOT: PSS was spin-coated on the Ni grid film with a thickness of 90 nm and energy dispersive spectroscopy (EDS) performed to investigate the elemental distribution of the composite film (Figs. 1(d) and 1(e)) clearly reveal the honeycomb and homogeneous distribution of elements Ni and S in the sample with regard to the metal grid and the PEDOT: PSS, respectively. As for the semi-solid hydrogel, it was quite soft and transparent (Fig. 1(f)), meanwhile, the mobile lithium chloride electrolyte endows the hydrogel with a high ionic conductivity and a red LED could be lightened in a circuit connected by it (Fig. 1(g)), demonstrating the multi-functionalities of the hydrogel in terms of ion storage, ion transportation and counter-conducting. In order to ensure the color contrast of the ECD between the coloring and bleaching states, the optical transmittance superiority in the electrode and hydrogel layers is very important and the simple triple-layered structure could decrease optical loss to a great extent. In addition, the triple-layered device has a better mechanical stability due to robust contact among the three functional layers under repeated bending. As for the hydrogel, the volatilization of water would narrow the channels of the 3D polymer network structure and reduce the ion mobility, and the long-term performance of the device could be improved by sealing the device by encapsulation. The transmittance spectra for the Ni grid electrode, the hydrogel, the ITO/glass and the ITO/PET are shown in Fig. 1(h). The multi-functional hydrogel electrode displays the highest transparency (~95%) in a wide wavelength range, due to its low refractive index and good film properties. The Ni grid electrode film and the ITO/glass exhibit similar optical transmittance (~84%), while the ITO/PET shows a significant decrease in transmittance, probably due to the PET deterioration under the stringent ITO fabrication conditions. In addition, the sheet resistance of the Ni grid electrode is 0.5 Ω/sq, indicating a figure of merit as high as 4383, which is advantageous for fabricating high

Optics EXPRESS

performance ECDs. The sheet resistance as a function of bending cycles for the Ni grid electrode and the ITO/PET film in Fig. 1(i) implies that the conducting properties of the electroplated Ni grid film is quite stable over a bending number of 2000, further demonstrating the suitability of the novel grid electrode for flexible ECDs. The Ni grid electrode could be designed into different patterns for displaying particular information by the flexible ECD. Figure 1(j) presents the images of a propitious cloud patterned ECD in the bleaching and coloring states (See Visualization 1).This also verifies that the grid electrode is an essential component in constructing the device, although the PEDOT: PSS layer also is conductive.

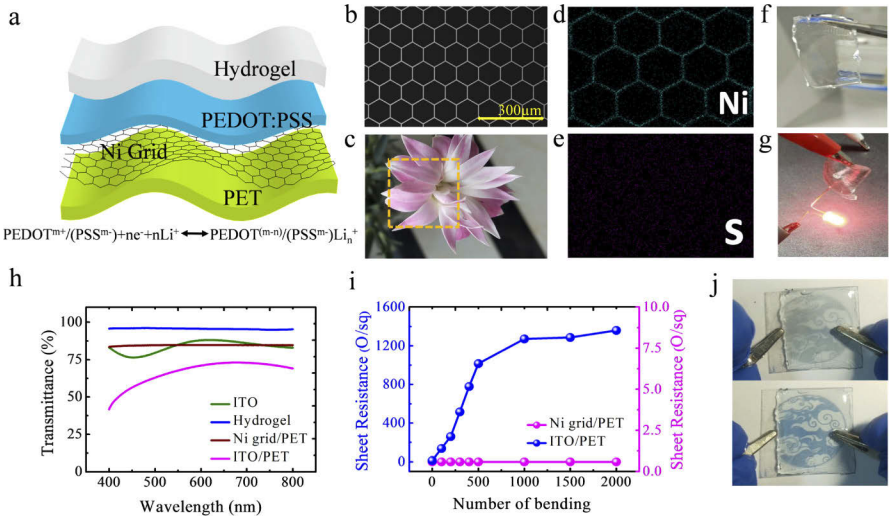

Fig. 1. (a) Illustration of the flexible ECD with simple triple-layered structure. (b) SEM image of the Ni grid electrode. (c) A flower image taken behind the Ni grid electrode. The yellow square denotes the electrode region. EDS mapping of (d) Ni element and (e) S element in the composite grid electrode/PEDOT: PSS film. (f) An image of the semi-solid hydrogel. (g) An image of a LED connected with the hydrogel in series. (h) The transmittance spectra of the ITO glass (green), the flexible ITO PET (purple), the Ni electrode (brown) and the hydrogel (blue) in the UV-Vis-NIR range. (i) Sheet resistance as a function of bending cycles for the Ni grid electrode (purple) and the flexible ITO PET (blue) with the bending radius of 0.5 cm. (j) Photographs of the bleached and colored state of propitious cloud using the flexible ECD with a patterned Ni grid electrode.

The excellent performance of the Ni grid electrode and the hydrogel in terms of the optical, electrical and mechanical properties, together with the simple working structure, would enable flexible ECDs with satisfying operating characteristics. Application of a voltage (negative bias to PEDOT: PSS) to the simple device switches the oxidation states of the PEDOT: PSS polymers so that the material is colored. Figure 2(a) shows the photographs of such a device as a function of the applied voltage and the transmittance spectra are provided in Fig. 2(b). The degree of the redox reaction increases as the applied voltage increases, resulting a higher optical absorption. The absorption of the EC material and thus the transmittance of the device can be continuously tuned and the maximum transmittance change was 40% at 650 nm with an operation voltage of 2 V, while the ITO PET based device comprising the same EC material has a maximum transmittance change of 28%, indicating the compatibility and superiority of the Ni grid electrode in these ECDs. Under the influence of alternating positive and negative electric fields, Li^+ and e^- were simultaneously injected and extracted in PEDOT: PSS layer, which induces the oxidation and reduction of the EC material, resulting in an alternation of coloring and fading states with

Optics EXPRESS

optical contrast. The PEDOT: PSS layer thickness was optimized in terms of the transmittance of the colored and bleached states to obtain a high optical contrast.

Figure 2(c) shows electrochromic switching behaviors of the device at 650 nm with a voltage of 1 V for 7 s and −2 V for 8 s for 16 cycles where the optical transmittance alternately changes. It can be further seen from Fig. 2(d) that the coloring time to reach 90% of the highest contrast is about 2.7 s and the corresponding bleaching time is about 4.7 s. When compared with the flexible ITO (See **Appendix** Fig. 5), the electrochromic device based on the Ni grid electrode has slightly faster response, because the Ni grid motif can provide direct electrical pathways for electrons and improve the electron transport rate to speed up the switching process. Without the application of the bleaching voltage, the EC material would return back to the neutral state with a relaxation time of around 3 min and suitable chemical modification of the conjugated polymer molecular structure may elongate the relaxation time and pave the way for bi-stable EC devices aiming for ultra-low power consumption smart windows. The long-term performance stability concerning the optical contrast and switching behaviors of the device was investigated in Figs. 2(e) and 2(f). The transmittance changes ΔT gradually decreased from 40% to 32% (about 80% contrast retention) after 1000 working cycles, and with a further increase in the recycling number, this working characteristic remained almost constant (See **Appendix** Fig. 6). The degradation of the transmittance modulation may be assigned to ion-trapping in the deep traps of the electrochromic material, which renders the reversible color change reaction difficult to be carried out. As for the switching characteristics, the coloring time increased from 2.7 s to 4.4 s and the bleaching time increased from 4.7 s to 6.4 s, probably due to the evaporation of liquid electrolyte in the hydrogel during the long working term. These results confirm that the Ni grid electrode is more stable than the Au grid and is almost free from oxidation and corrosion even without any protection layer [35].

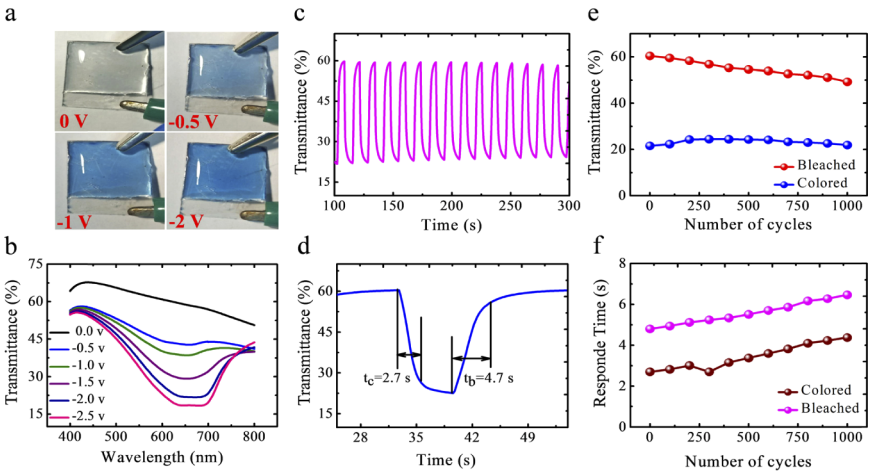

Fig. 2. Electrochromic performance of the ECD. (a) Photographs of the device at different coloration voltages. (b) Transmission spectra of the ECD at different coloring states. (c) The switching characteristics of the ECD, where the coloring and bleaching voltage was −2 V and 1 V, respectively. (d) Optical responses for coloring and bleaching steps. (e) The transmittance of the ECD at 650 nm as a function of the operation cycles at the bleaching and coloring states. (f) The response time as a function of the operation cycles for the bleaching and coloring steps.

Due to the high electron and ion conductivity of the Ni grid electrode and the semi-solid hydrogel, the simple triple-layered device exhibits good electrochromic performance in terms of the optical contrast and the switching speed. Apart from this, the Ni grid electrode and the

Optics EXPRESS

transparent hydrogel also have the advantage of mechanical flexibility and the intact surface contact among these three layers is also beneficial to fabricate the flexible ECD. In order to demonstrate the potential of the device for wearable electronics, the ECD was conformably attached to bottles with different radii. The switching behaviors of the device at different bending radii are shown in Fig. 3 and the photographs of the sample in the bleaching and coloring states at the corresponding bending radius are also given in the lower panel. A video presenting a dynamic operation of the device at the bending state was also provided in the supplementary material (See Visualization 2). The conformably attached device preserves satisfying electrochromic characteristics in terms of the optical contrast and the switching speed, indicating that the electrochromic device is very flexible without performance degradation. The transmittance at the bleaching and coloring states become lower at the higher bending curvature, due to the increased tested area and optical loss including scattering, reflection and absorption.

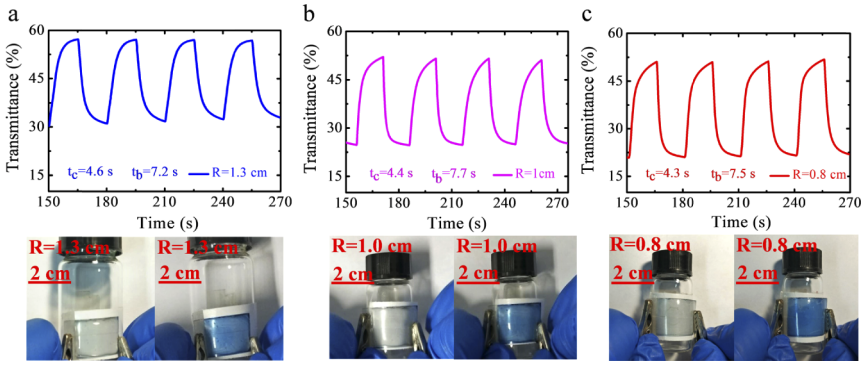

Fig. 3. Switching performance of the ECD at a bending radius of 1.3 cm (a), 1 cm (b) and 0.8 cm (c), respectively. The transmission spectra were monitored at the wavelength of 650 nm. The low panel are photographs of samples in bleached and colored states at the corresponding bending radius.

To further evaluate the mechanical flexibility and reliability of the electrochromic device, the triple-layered device was repeatedly bent to a radius of 0.5 cm and the in situ electrochromic behaviors during the bending test were measured by the spectrometer and the electrochemical workstation. The transmittance spectrum in the UV-VIS-NIR and the dynamic switching performance at 650 nm as a function of the bending cycles was shown in Figs. 4(a) and 4(b), respectively. The characteristic absorption peak remains the same, albeit with an attenuation in the intensity, resulting in a slight degradation in the optical contrast. From Fig. 4(c), the optical transmittance of the bleaching state remains almost constant during the bending, while that of the colored state experiences a slight decrease, and this may probably due to the detachment of the electrochromic material from the Ni grid electrode or the non-uniform conformal contact between the PEDOT: PSS layer and the hydrogel after the bending cycles. However, the results in Fig. 4(c) show that the ΔT (the transmittance contrast between the colored (−2 V) and bleached (0 V) state) remained around 87.5% of the initial value (from 40% to 35%) after 1000 bending cycles, and still, after 2500 bending cycles the transmittance contrast preserves as high as 30.4% (Corresponding to 76% retention). The bending performance of the triple-layered device is comparable to the flexible ECD based on Ag and $W_{18}O_{49}$ nanowire assemblies [22], and could be further improved by reducing the thickness of the PET substrate and the thickness of the hydrogel, as predicted by the significantly mitigated strain difference. As for the switching time, the coloring time increased slightly from 2.7 s to 4.3 s while the bleaching time first exhibited a fast increase from 4.7 s to 7.3 s in the initial 1000 bending cycles and remain almost constant with further bending operations (Fig. 4(d)). The different dependence of the switch

Optics EXPRESS

behaviors on bending cycles could be explained by the different influences of the bending on the processes of intercalation and deintercalation, where the device bending may result in defects in the PEDOT: PSS material which act as the traps for ions. In general, the device preserves satisfying electrochromic performance after a number of bending cycles, which is promised to be used in conformable smart windows and wearable devices.

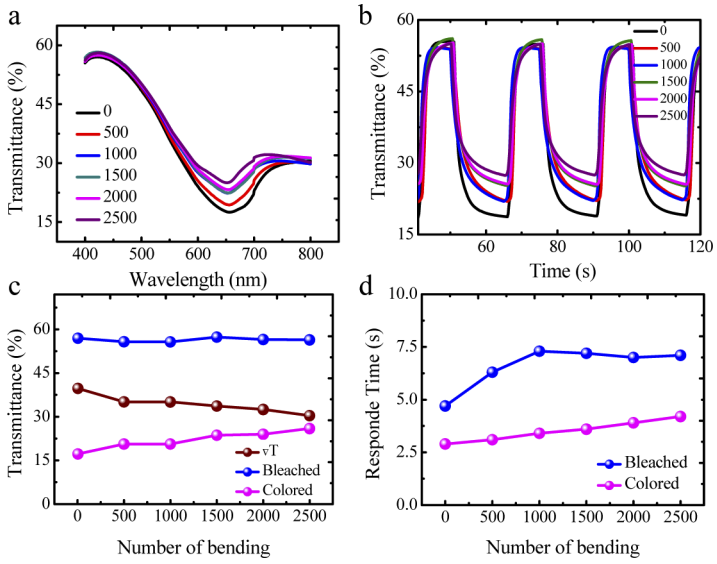

Fig. 4. Electrochromic performance of the ECD as a function of the bending cycles. (a) The transmission spectra of ECD in the coloring state after 0, 500, 1000, 1500, 2000, and 2500 bending cycles. (b) Switching behaviors of the ECD at 650 nm after 0, 500, 1000, 1500, 2000, and 2500 bending cycles. (c) The dependence of bleached transmittance, colored transmittance and transmittance change at 650 nm on the bending cycles. (d) The dependence of the bleaching time and the coloring time on the bending cycles. The coloring voltage is −2 V, and the bleaching voltage is 1 V.

4. Conclusion

In summary, we have presented a new flexible electrochromic device enabled by the electroplated Ni grid electrode and the multifunctional hydrogel. Compared with previous flexible electrochromic devices on ITO or silver nanowire, the Ni grid electrode has advantages of high conductivity, high optical transmittance, high mechanical flexibility and high stability from oxidation, which guarantee the fabrication of the novel high-performance device. In addition, the hydrogel is multi-functional in terms of ion storage, ion transportation and counter-conducting and is beneficial to construct a very simple electrochromic device with a triple-layered architecture, thereby simplifying the fabrication process and improving the device flexibility. The electrochromic device presents a transmittance contrast of 40% with a coloration time of 2.7 s at −2 V and a bleaching time of 4.7 s at 1 V, and good performance retention on conformal attaching and a bending cycle number of 2500, opening a way for highly flexible and reliable electrochromic devices with volume manufacturing potential.

Optics EXPRESS

A. Appendix

A.1. Electrochromic performance of the device on a flexible ITO substrate

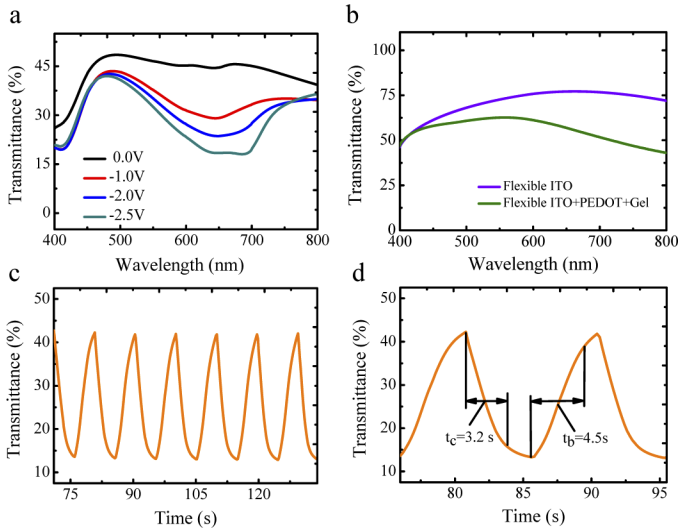

Fig. 5. Electrochromic performance of the ECD on the flexible ITO substrate. (a) The transmittance spectra of the flexible ITO PET (purple) and the completed ECD at the bleaching state (green) in the UV-Vis-NIR range. (b) Transmission spectra of the device at different coloring states. (c) The switching characteristics of the device at 650 nm, where the coloring and bleaching voltage was −2 V and 1 V, respectively. (d) Optical responses for coloring and bleaching steps at 650 nm.

A.2. Long-term switching performance of the electrochromic device based on the Ni grid electrode

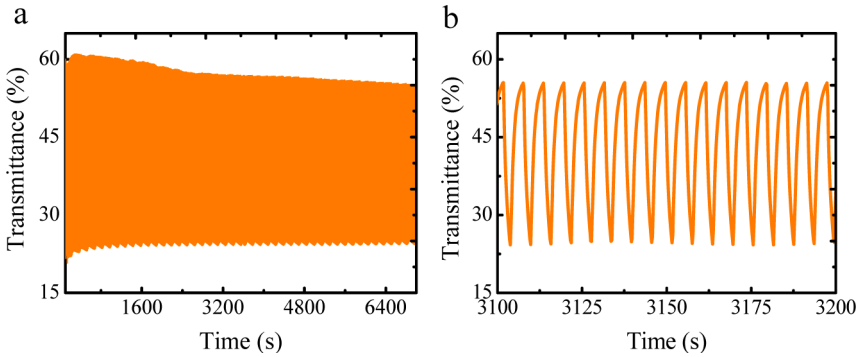

Fig. 6. The switching characteristics of our device at 650 nm (a) up to an operation cycle number over 3200, where the absolute transmittance contrast first decreases and then flattens; (b) in stable manner with an operation cycle number between 1000 and 1100. The coloring and bleaching voltage was −2 V and 1 V, respectively.

Optics EXPRESS

Funding

National Natural Science Foundation of China (61505131, 61575135); Natural Science Foundation of Jiangsu Province (BK20181166); China Postdoctoral Science Foundation (2017T100403); Natural Science Research of Jiangsu Higher Education Institutions of China (18KJB510040).

References

1. Z. Liu, J. Xu, D. Chen, and G. Shen, "Flexible electronics based on inorganic nanowires," Chem. Soc. Rev. **44**(1), 161–192 (2015).
2. J. A. Rogers, T. Someya, and Y. Huang, "Materials and mechanics for stretchable electronics," Science **327**(5973), 1603–1607 (2010).
3. A. L. S. Eh, A. W. M. Tan, X. Cheng, S. Magdassi, and P. S. Lee, "Recent advances in flexible electrochromic devices: prerequisites, challenges, and prospects," Energy Technol. **6**(1), 33–45 (2018).
4. S. G. Lee, D. Y. Lee, H. S. Lim, D. H. Lee, S. Lee, and K. Cho, "Switchable transparency and wetting of elastomeric smart windows," Adv. Mater. **22**(44), 5013–5017 (2010).
5. E. L. Runnerstrom, A. Llordés, S. D. Lounis, and D. J. Milliron, "Nanostructured electrochromic smart windows: traditional materials and NIR-selective plasmonic nanocrystals," Chem. Commun. **50**(73), 10555–10572 (2014).
6. P. Tehrani, L.-O. Hennerdal, A. L. Dyer, J. R. Reynolds, and M. Berggren, "Improving the contrast of all-printed electrochromic polymer on paper displays," J. Mater. Chem. **19**(13), 1799–1802 (2009).
7. W. Weng, T. Higuchi, M. Suzuki, T. Fukuoka, T. Shimomura, M. Ono, L. Radhakrishnan, H. Wang, N. Suzuki, H. Oveisi, and Y. Yamauchi, "A high-speed passive-matrix electrochromic display using a mesoporous TiO2 electrode with vertical porosity," Angew. Chem., Int. Ed. **49**(23), 3956–3959 (2010).
8. L. X. YingZhu, T. Chang, J. Bell, A. Huang, P. Jin, and S. Bao, "High performance all-solid-state electrochromic device based on LixNiOy layer with gradient Li distribution," Electrochim. Acta **317**, 10–16 (2019).
9. J. Jensen and F. C. Krebs, "From the bottom up-flexible solid state electrochromic devices," Adv. Mater. **26**(42), 7231–7234 (2014).
10. A. Bessière, J.-C. Badot, M.-C. Certiat, J. Livage, V. Lucas, and N. Baffier, "Sol-gel deposition of electrochromic WO3 thin film on flexible ITO/PET substrate," Electrochim. Acta **46**(13-14), 2251–2256 (2001).
11. C. M. White, D. T. Gillaspie, E. Whitney, S.-H. Lee, and A. C. Dillon, "Flexible electrochromic devices based on crystalline WO3 nanostructures produced with hot-wire chemical vapor deposition," Thin Solid Films **517**(12), 3596–3599 (2009).
12. L. Liang, J. Zhang, Y. Zhou, J. Xie, X. Zhang, M. Guan, B. Pan, and Y. Xie, "High-performance flexible electrochromic device based on facile semiconductor-to-metal transition realized by WO3·2H2O ultrathin nanosheets," Sci. Rep. **3**(1), 1936 (2013).
13. H.-J. Yen, C.-J. Chen, and G.-S. Liou, "Flexible multi-colored electrochromic and volatile polymer memory devices derived from starburst triarylamine-based electroactive polyimide," Adv. Funct. Mater. **23**(42), 5307–5316 (2013).
14. A. Aliprandi, T. Moreira, C. Anichini, M. A. Stoeckel, M. Eredia, U. Sassi, M. Bruna, C. Pinheiro, C. A. T. Laia, S. Bonacchi, and P. Samorì, "Hybrid copper-nanowire–reduced-graphene-oxide coatings: a "green solution" toward highly transparent, highly conductive, and flexible electrodes for (opto)electronics," Adv. Mater. **29**(41), 1703225 (2017).
15. K. Zhou, H. Wang, J. Jiu, J. Liu, H. Yan, and K. Suganuma, "Polyaniline films with modified nanostructure for bifunctional flexible multicolor electrochromic and supercapacitor applications," Chem. Eng. J. **345**, 290–299 (2018).
16. A. A. Argun, A. Cirpan, and J. R. Reynolds, "The first truly all-polymer electrochromic device," Adv. Mater. **15**(16), 1338–1341 (2003).
17. R. Singh, J. Tharion, S. Murugan, and A. Kumar, "ITO-free solution-processed flexible electrochromic devices based on PEDOT: PSS as transparent conducting electrode," ACS Appl. Mater. Interfaces **9**(23), 19427–19435 (2017).
18. L. V. Kayser and D. J. Lipomi, "Stretchable conductive polymers and composites based on PEDOT and PEDOT:PSS," Adv. Mater. **31**(10), 1806133 (2019).
19. S. Lin, X. Bai, H. Wang, H. Wang, J. Song, K. Huang, C. Wang, N. Wang, B. Li, M. Lei, and H. Wu, "Roll-to-roll production of transparent silver-nanofiber-network electrodes for flexible electrochromic smart windows," Adv. Mater. **29**(41), 1703238 (2017).
20. L. Shen, L. Du, S. Tan, Z. Zang, C. Zhao, and W. Mai, "Flexible electrochromic supercapacitor hybrid electrodes based on tungsten oxide films and silver nanowires," Chem. Commun. **52**(37), 6296–6299 (2016).
21. C. Lee, Y. Oh, I. S. Yoon, S. H. Kim, B.-K. Ju, and J.-M. Hong, "Flash-induced nanowelding of silver nanowire networks for transparent stretchable electrochromic devices," Sci. Rep. **8**(1), 2763 (2018).
22. J.-L. Wang, Y.-R. Lu, H.-H. Li, J.-W. Liu, and S.-H. Yu, "Large area co-assembly of nanowires for flexible transparent smart windows," J. Am. Chem. Soc. **139**(29), 9921–9926 (2017).
23. W. Kang, M.-F. Lin, J. Chen, and P. S. Lee, "Highly transparent conducting nanopaper for solid state foldable electrochromic devices," Small **12**(46), 6370–6377 (2016).
24. T. G. Yun, M. Park, D.-H. Kim, D. Kim, J. Y. Cheong, J. G. Bae, S. M. Han, and I.-D. Kim, "All-transparent stretchable electrochromic supercapacitor wearable patch device," ACS Nano **13**(3), 3141–3150 (2019).

Optics EXPRESS

25. K. Mallikarjuna and H. Kim, "Highly transparent conductive reduced graphene oxide/silver nanowires/silver grid electrodes for low-voltage electrochromic smart windows," ACS Appl. Mater. Interfaces **11**(2), 1969–1978 (2019).
26. C. Chen, Y. G. Jia, D. Jia, S. X. Li, S. L. Ji, and C. H. Ye, "Formulation of concentrated and stable ink of silver nanowires with applications in transparent conductive films," RSC Adv. **7**(4), 1936–1942 (2017).
27. C. Chen, Y. Zhao, W. Wei, J. Q. Tao, G. W. Lei, D. Jia, M. J. Wan, S. X. Li, S. L. Ji, and C. H. Ye, "Fabrication of silver nanowire transparent conductive films with an ultra-low haze and ultra-high uniformity," J. Mater. Chem. C **5**(9), 2240–2246 (2017).
28. C. Chen, Z. C. Huang, Y. L. Jiao, Y. Y. Zhang, J. W. Li, C. Z. Li, X. D. Lv, S. H. Wu, Y. L. Hu, W. L. Zhu, D. Wu, J. R. Chu, and L. Jiang, "In-situ reversible control between sliding and pinning for diverse liquids under ultralow voltage," ACS Nano **13**(5), 5742–5752 (2019).
29. G. Cai, P. Darmawan, M. Cui, J. Wang, J. Chen, S. Magdassi, and P. S. Lee, "Highly stable transparent conductive silver grid/PEDOT:PSS electrodes for integrated bifunctional flexible electrochromic supercapacitors," Adv. Energy Mater. **6**(4), 1501882 (2016).
30. M. Layani, P. Darmawan, W. L. Foo, L. Liu, A. Kamyshny, D. Mandler, S. Magdassi, and P. S. Lee, "Nanostructured electrochromic films by inkjet printing on large area and flexible transparent silver electrodes," Nanoscale **6**(9), 4572–4576 (2014).
31. L. Liu, M. Layani, S. Yellinek, A. Kamyshny, H. Ling, P. S. Lee, S. Magdassi, and D. Mandler, ""Nano to nano" electrodeposition of WO3 crystalline nanoparticles for electrochromic coatings," J. Mater. Chem. A **2**(38), 16224–16229 (2014).
32. G. Cai, X. Cheng, M. Layani, A. W. M. Tan, S. Li, A. Eh, D. Gao, S. Magdassi, and P. S. Lee, "Direct inkjet-patterning of energy efficient flexible electrochromics," Nano Energy **49**, 147–154 (2018).
33. J. Jensen, M. Hösel, I. Kim, J.-S. Yu, J. Jo, and F. C. Krebs, "Fast switching ITO free electrochromic devices," Adv. Funct. Mater. **24**(9), 1228–1233 (2014).
34. R. R. Søndergaard, M. Hösel, M. Jørgensen, and F. C. Krebs, "Fast printing of thin, large area, ITO free electrochromics on flexible barrier foil," J. Polym. Sci., Part B: Polym. Phys. **51**(2), 132–136 (2013).
35. T. Qiu, B. Luo, M. Liang, J. Ning, B. Wang, X. Li, and L. Zhi, "Hydrogen reduced graphene oxide/metal grid hybrid film: towards high performance transparent conductive electrode for flexible electrochromic devices," Carbon **81**, 232–238 (2015).
36. Y. Kim, H. Shin, M. Han, S. Seo, W. Lee, J. Na, C. Park, and E. Kim, "Energy saving electrochromic polymer windows with a highly transparent charge-balancing layer," Adv. Funct. Mater. **27**(31), 1701192 (2017).
37. C. Keplinger, J.-Y. Sun, C. C. Foo, G. M. Whitesides, and Z. Suo, "Stretchable, transparent, ionic conductors," Science **341**(6149), 984–987 (2013).
38. H. Kai, W. Suda, Y. Ogawa, K. Nagamine, and M. Nishizawa, "Intrinsically stretchable electrochromic display by a composite film of poly (3, 4-ethylenedioxythiophene) and polyurethane," ACS Appl. Mater. Interfaces **9**(23), 19513–19518 (2017).
39. H. Fang, P. Zheng, R. Ma, C. Xu, G. Yang, Q. Wang, and H. Wang, "Multifunctional hydrogel enables extremely simplified electrochromic devices for smart windows and ionic writing boards," Mater. Horiz. **5**(5), 1000–1007 (2018).
40. Y.-H. Liu, J.-L. Xu, X. Gao, Y.-L. Sun, J.-J. Lv, S. Shen, L.-S. Chen, and S.-D. Wang, "Freestanding transparent metallic network based ultrathin, foldable and designable supercapacitors," Energy Environ. Sci. **10**(12), 2534–2543 (2017).